9-2020

A comparison of the area of the internal nasal valve in CBCT and MRI

Chantelle Ghiam

LOMA LINDA UNIVERSITY
School of Dentistry
in conjunction with the
Faculty of Graduate Studies

A comparison of the area of the internal nasal valve in CBCT and MRI

by

Chantelle Ghiam

A Thesis submitted in partial satisfaction of
the requirements for the degree
Master of Science in Orthodontics and Dentofacial Orthopedics

---

September 2020

Each person whose signature appears below certifies that this thesis in his/her opinion is adequate, in scope and quality, as a thesis for the degree Master of Science.

_____, Chairperson
V. Leroy Leggitt, Professor of Orthodontics and Dentofacial Orthopedics

_____
James Farrage, Associate Professor of Orthodontics and Dentofacial Orthopedics

_____
Gina Roque-Torres, Assistant Professor, Center for Dental Research

ACKNOWLEDGEMENTS

I would like to express my deepest appreciation to the members of my research guidance committee: Dr. Leggitt, Dr. Farrage, and Dr. Roque-Torres for their constant encouragement and support. Thank you to Seth Myhre for technical support and to Udo Oyoyo, for providing statistical analysis. I would also like to thank Dr. Caruso and Dr. Jeiroudi for taking the time to review my protocol.

CONTENTS

FIGURES

Figures Page

TABLES

Tables Page

ABBREVIATIONS

2D	Two-dimensional
3D	Three-dimensional
3T	3-Tesla
ALARA	As Low As Reasonably Achievable
CBCT	Cone Beam Computed Tomography
CT	Computed Tomography
DICOM	Digital Imaging and Communications in Medicine
EAA	Estimated Acoustic Axis
FH	Frankfort Horizontal
FOV	Field of View
ICC	Intraclass Correlation Coefficient
INC	Inferior Nasal Concha
INV	Internal Nasal Valve
IRB	Institutional Review Board
LLUSD	Loma Linda University School of Dentistry
MR	Magnetic Resonance
MRI	Magnetic Resonance Imaging
Na	Nasion
PNS	Posterior Nasal Spine
sNa	Soft Tissue Nasion
TMJ	Temporomandibular Joint
TNB	Tip of the Nasal Bone

ABSTRACT OF THE THESIS

A comparison of the area of the internal nasal valve in CBCT and MRI

by

Chantelle Ghiam

Master of Science, Graduate Program in Orthodontics and Dentofacial Orthopedics
Loma Linda University, September 2020
Dr. V. Leroy Leggitt, Chairperson

Objective: This study compared the agreement between whole head Cone-Beam Computed Tomography (CBCT) and 3T Magnetic Resonance Imaging (MRI) methods to assess the cross-sectional area of the internal nasal valve.

Methods: Thirteen human subjects (mean age 15y11m) were used in this study. All scans were preformed within two weeks of one another. CBCT images were made with an 18x16 inch field of view, exposure time of 5.4 s, and resolution of 0.3x0.3x0.3 mm. 3T MR images were captured as contiguous sagittal images of the whole head with a T1-weighted 3D imaging sequence (Magnetization Prepared Rapid Acquisition by Gradient Echo (MP-RAGE), TP/TE = 1950/2.26 ms) and resolution of 1.0x1.0x1.0 mm. Simpleware Scan IP (v.M-2018.03) imaging software was used to process the images in the following order: 1) registration 2) airway segmentation, 3) cross-sectional area measurement. Agreement between CBCT and MRI measurements was evaluated with an Intraclass Correlation Coefficient (ICC). Intra-rater reliability (after a 1-month washout period) was also evaluated with an ICC. A Bland-Altman test was used to determine whether systematic or proportional bias was present.

Results: Excellent agreement between CBCT and MRI cross-sectional area measurements of the internal nasal valve was observed. Mean ICC was 0.876 (CI 0.833 – 0.908). Reliability was demonstrated with an ICC of 0.999 (CI 0.998 – 1.00) for MRI and an ICC of 1.00 (CI 1.00 – 1.00) for CBCT measurements. The degree of bias ranged from -0.068 - 0.123 cm^2. No statistically significant systematic ($p>0.05$) or proportional ($p>0.05$) bias was observed.

Conclusion: MRI and CBCT give similar cross-sectional area measurements of the internal nasal valve. These results indicate that further studies are necessary to evaluate the interchangeability of CBCT and MRI for the purpose of nasal airway analysis.

CHAPTER ONE

REVIEW OF THE LITERATURE

Introduction

Diagnostic imaging plays an essential role in the evaluation and treatment of patients for orthodontic purposes. It is a key factor that allows an orthodontist to accurately monitor a patient's progress throughout treatment. Conventional orthodontic imaging modalities include a panorex, lateral cephalogram, and full mouth x-rays. Conventional cephalometric radiography is limited in its application by the expression of 3D structures onto a 2D plane. As a result, the superimposition of anatomical structures interferes with landmark identification and can lead to magnification and distortion of the image obtained. These 2D imaging modalities pose considerable disadvantages, namely that they do not represent the full dimensions of the upper airway or the 3D development of craniofacial structures. 3D imaging modalities such as MRI, CBCT, and CT have been developed that can reduce the problems associated with 2D imaging. Of these 3D imaging modalities CBCT has become increasingly important in orthodontic treatment planning.

CBCT

Dental CBCT was introduced to replace medical CT for the craniofacial region and to lower the radiation dose to the patient.[1] In a study by Mozzo et al., it was concluded that the application of CBCT systems for imaging dentofacial structures is necessary due to increasing advancements in dentistry including, implant placement,

which require such an imaging modality.[2] CBCT has gained a widespread interest in orthodontics, providing accurate, high quality images at a relatively low cost. CBCT is now readily used as the preferred imaging modality in orthodontic diagnosis and treatment planning.[3]

In a review by Mah et al., it was concluded that the complexities of the craniofacial complex, dentition, and airway pose challenges in attaining conventional images and the application of CBCT can lead to improved visualization.[4] When comparing conventional radiography, Hodges et al., found that CBCT provides more information for locating pathology, identifying root resorption and accurate treatment planning.[5] CBCT displays 3D structures, allows multiplanar reconstructions and allows us to measure the volume and cross-sectional area of structures, providing a significant amount of diagnostic information.[3,4]

With the advent of CBCT, a 3D visualization of the craniofacial skeleton is clearly represented in all three planes-sagittal, coronal, and transverse. In a study by Ludlow et al., it was determined that multiplanar views are particularly useful in identifying bilateral landmarks such as orbitale, condylion, and gonion, which are commonly superimposed on conventional radiographs.[6] Applications of CBCT include the localization of impacted teeth, the evaluation of the temporomandibular joints, visualization of airway patency, and skeletal abnormalities.[4,5,7] Thus, CBCT has become an exceptional tool for accurate diagnosis, predictable treatment planning, more effective patient management and education, and enhanced treatment outcome and patient satisfaction.

While it provides significant advantages to conventional radiography, patients undergoing CBCT scans are exposed to ionizing radiation. Consequently, the gains in diagnostic accuracy must outweigh the risks of radiation exposure to be deemed acceptable. CBCT radiation doses are significantly higher than normal dental radiography, which precludes its use in routine examination. Grunheid et al., preformed a study that compared CBCT scans and conventional radiography commonly used in orthodontics. They found the effective dose for panoramic radiography to be about 21.5 microsieverts and for a lateral cephalogram to be about 4.5 microsieverts. The effective radiation dose for CBCT scan ranged from 64.7 to 134.2 microsieverts.[8] So, although CBCT provides diagnostic advantages, it also exposes patients to higher levels of ionizing radiation. To determine if CBCT scans can justifiably be utilized for orthodontic patients, additional research concerning patient safety is required.

The American Dental Association (ADA) states that radiation procedures like CBCT must be used sparingly and only for situations that are deemed necessary for diagnosis. Radiation exposure should be as low as reasonably achievable (ALARA), a principle to help guide healthcare professionals in deciding when dental radiography is considered necessary.[9] The guidelines highlight the importance of taking radiographs based upon patient's needs, and the images obtained should serve a diagnostic purpose.

MRI

Another imaging technique available to medical professionals is Magnetic Resonance Imaging (MRI). MRI is another form of 3-D imaging that uses non-ionizing electromagnetic radiation. The advantages of MRI include but are not limited to, the

ability to visualize the TMJ and articular disk, display soft and hard tissue, localize impacted teeth, and assess the airway.[10] MRI has a much higher resolution for soft tissues subsequently allowing the visualization of the position and morphology of the articular disk, rendering MRI as the gold standard for TMJ imaging.[11] In a prospective study by Tymofiyeva et al., found that impacted teeth were clearly distinguishable from adjacent tissues in an MRI scan and the angulation and position of the teeth could be determined in three dimensions.[12] The study shows that MRI gives us valuable information without the need for ionizing radiation in essence maximizing the effect of the ALARA principle. The ability to use MRI in orthodontic diagnosis and treatment planning could be a significant advancement towards minimizing the patient's exposure to ionizing radiation.

The mechanism of creating an MRI image involves recording a resonance signal from the excited hydrogen atoms created by a magnetic field. The magnetic field is the scanner, which surrounds the patient and gradient coils are switched on and off to change the magnetic field. As the magnetic field excites atoms, an equilibrium state energy is sensed. The energy is converted to a number, which is processed by a computer and an image is then created. In essence, MRI images the water content in the tissues, and since different tissues have different water contents, a detailed image is generated that clearly distinguishes the various tissues.

In a study by Xiong et al., a 3D structure of the upper airway was constructed based on magnetic resonance imaging. It was concluded that the volume and area of every cross section of the upper airway can be measured from the constructed 3D model of the upper airway with improved accuracy.[13] The study indicates that MRI provides valuable information about the airway without the need for ionizing radiation. In a

preliminary study by Tai et al., that explored the 3D accuracy of registered MRI and CBCT images, found that there were no significant linear measurement errors when the images were measured from the superimposed MRI-CBCT images. The study concluded that MRI and CBCT images showed similar linear measurements.[14]

Nevertheless, certain disadvantages persist with the use of MRI, including higher costs, limited accessibility to dental professionals, discomfort to claustrophobic patients, and limited visibility of hard tissues. Additionally, the presence of most metal objects in the body is contraindicated in patients acquiring an MRI scan, posing a potential problem for patients who are undergoing orthodontic treatment. All patients must be thoroughly screened prior to an MRI scan.

Potential Effect on Craniofacial Development

Obstruction of the upper airway and consequent mouth breathing can negatively impact the craniofacial structures and the developing dentition. Orthodontists must play an active role in managing airway development and craniofacial maturation in growing children. In a review by Rojas et al., it was concluded that upper airway assessment including a radiographic evaluation and CBCT scan is essential to help identify functional changes that could interfere with orthodontic treatment. Research has strongly suggested that craniofacial malformation can lead to airway obstruction, impaired respiration and nasal breathing, chronic mouth breathing, sleep apnea, and long-term poor quality of life.[15-18] Orthodontic and orthopedic treatments have the potential to improve the nasal airway and positively impact breathing, leading to a healthier overall life.

Anatomy

The normal airway begins from a functional standpoint in the nostrils. The nasal airway includes the nares, the nasal cavities, and extends posteriorly to the nasopharynx. The nasal valve area can be divided into the external and internal nasal valve. The external nasal valve is the region bordered by the nostril opening caudally, the septum medially, and the alar cartilage laterally. Located 1.3 cm deep to the nares, the internal nasal valve is bordered medially by the dorsal septum, laterally by the caudal margin of the upper lateral cartilage, and inferiorly by the head of the inferior turbinate.[19]

Significance of the Internal Nasal Valve

The internal nasal valve is the narrowest area of the nasal cavity and the site of maximum resistance along the entire respiratory tract. Any narrowing of the nasal valve size and collapse can lead to significant airway resistance.[19] Common causes of nasal valve collapse include rhinoplasty, a deviated septum, or trauma to the nose. A study by Ribault et al., demonstrated that major nasal obstruction was four times more common in the group of children with orthodontic abnormalities.[18] Early prevention of nasal incompetence in children and its timely treatment are essential for proper craniofacial growth and ensure the long-term stability of orthodontic treatment.

The internal nasal valve forms an important anatomical landmark. A study done by Murthy et al., presented evidence that narrowing of the internal nasal valve will have a significant effect on sinus and middle ear pathology.[19] Prolonged oral breathing commonly results in dental and skeletal malformation in growing children. In a study by Principato et al., the authors concluded that some of the adverse consequences of chronic

oral breathing include unwanted molar eruption, increased anterior vertical face height, retrognathia, and open bite. These commonly associated problems may also lead to low tongue posture, a constricted maxillary arch, and a retrognathic maxilla.[17] Another study by Lopatiene et al., showed a significant association between nasal resistance and increased overjet, open bite and maxillary crowding.[16] The Clinical consensus statement, released in the *Journal of Otolaryngology-Head and Neck Surgery* in 2010, established Nasal Valve Collapse as a diagnosable condition with specific treatments options to restore function.

Internal Nasal Valve Imaging Modalities

Several studies have aimed to evaluate the internal nasal valve using standard computed tomography (CT) imaging. CT scans has been proposed as an objective tool to measure internal nasal valve morphology.[20,21] A study by Moche et al., presented evidence for using standard axial CT imaging as an objective method of radiographically evaluating the nasal valve, demonstrating a strong correlation with physical examination and patient complaint. It was concluded that radiographic valve areas can be used to screen for clinically narrow nasal valves with good sensitivity and specificity.[22] Another opinion was offered by, Veron et al., who concluded that CT analysis of the anatomy of the nasal valve is currently not accepted as an objective system in clinical nasal incompetence.

As the site of greatest airflow resistance within the nasal airway, the internal nasal valve may be of great importance when assessing airway patency. Although a number of studies have measured the valve area in standard CT imaging, there are few CBCT and

MRI imaging studies designed to measure the nasal valve area. The purpose of this study was to determine the agreement between internal nasal valve measurements made on 3T MR and CBCT scans. The ability to use MRI to accurately assess the airway would be of great value since it would eliminate patients' exposure to ionizing radiation.

CHAPTER TWO

MEASUREMENTS OF THE INTERNAL NASAL VALVE USING WHOLE HEAD 3T MRI AND CBCT

Introduction

Conventional orthodontic imaging modalities include a panorex, lateral cephalogram, and full mouth x-rays. However, these 2D imaging modalities pose considerable disadvantages, namely that they do not represent the full dimensions of the upper airway or the 3D development of craniofacial structures. Consequently, geometric distortion, superimposition of anatomical structures, and magnification inaccuracies occur.[1,6] 3D imaging modalities such as MRI, CBCT, and CT have been developed that can reduce the problems associated with 2D imaging. Of these 3D imaging modalities CBCT has become increasingly important in orthodontic treatment planning.

CBCT is now the preferred imaging modality in orthodontic diagnosis and treatment planning.[3] CBCT displays 3D structures, allows multiplanar reconstructions, and allows us to measure the volume and cross-sectional area of structures, providing a significant amount of diagnostic information.[3,4] Applications of CBCT include the localization of impacted teeth, the evaluation of the temporomandibular joints, visualization of airway patency, and skeletal abnormalities.[4,5,7] However, CBCT radiation doses are significantly higher than normal dental radiography, which precludes its use in routine examination.[8] Long-term exposure to ionizing radiation has proven to have carcinogenic effects, thus utilizing other imaging modalities may reduce such risks and maximize the effect of the ALARA principle.[9]

In contrast to CBCT, MRI uses non-ionizing electromagnetic radiation. MRI allows for repetitive 3-D imaging of craniofacial structures without the potential detrimental effects of radiation exposure.[11] The advantages of MRI include but are not limited to, the ability to visualize the TMJ and disk, display soft and hard tissue, localize impacted teeth, and assess the airway.[10]

Nevertheless, certain disadvantages persist with the use of MRI, including higher costs, limited accessibility to dental professionals, discomfort to claustrophobic patients, and limited visibility of hard tissues. Additionally, the presence of most metal objects in the body is contraindicated in patients acquiring an MRI scan, posing a potential problem for patients who are undergoing orthodontic treatment.

Although MRI provides detailed images of the craniofacial structures without exposing the patient to ionizing radiation, it has not been adopted as a viable imaging technique in the field of orthodontics. The ability to use MRI to accurately assess the airway would be of great value since it would eliminate patients' exposure to ionizing radiation and consequently reduce the harmful effects it comes with.

The purpose of this study was to determine the agreement between internal nasal valve measurements made on 3T MR and CBCT scans. This study tested the hypothesis that the measured cross-sectional area of the internal nasal valve acquired from MRI scans will be no different than those retrieved from CBCT scans. This research will provide valuable information to determine the accuracy of assessing a clinically significant area of the airway, which can shed light on the prospect of transitioning from CBCT to MRI in the future.

Materials and Methods

Patient Selection

This retrospective study evaluated measurements made on CBCT and MR scans of thirteen subjects. The subjects age ranged from 12 years and 1 month to 31 years and 5 months, with the average age being 15 years and 11 months. Seven subjects were male and six were female. Patients were selected based on their agreement to participate in the study and on the lack of exclusion criteria. Exclusion criteria included the presence of: 1) metal dental restorations, 2) dental implants, 3) fixed orthodontic appliances, 4) removable orthodontic appliances, 5) pacemakers, 6) cochlear implants, 7) metal foreign bodies in the eyes, 8) aneurysm clips, 9) prosthetic metal implants, 10) pregnancy.

Image Acquisition

One CBCT scan (NewTom, 5G, AFP Imaging, USA) and one 3T MR scan (Siemens Medical Solutions, DE) without intraoral contrast media was performed on each subject. All scans were preformed within two weeks of one another, prior to the placement of orthodontic separators or appliances. CBCT images were acquired with a 18x16 inch field of view that covered the entire head. Contiguous sagittal MR images of the whole head were created in a 3.0T imaging system with a T1-weighted 3D imaging sequence (Magnetization Prepared Rapid Acquisition by Gradient Echo (MP-RAGE), TR/TE = 1950/2.26 ms) and isotropic resolution of 1.0x1.0x1.0 mm. Scan time was less than 4 minutes.

Captured images of the internal nasal valve were exported in Digital Imaging and

Communications in Medicine (DICOM) format.

Superimposition

For the measurements of the internal nasal valve, the CBCT and MRI images were imported as DICOM files into Simpleware, Scan IP: 2018-03 (Exeter, United Kingdom) which allows for segmentation and calculation of the area of a 3D volume.

The CBCT and MRI files were registered together so that both images were superimposed. Registration was accomplished using nasion, pogonian and the apex of the central incisor. Registration and superimposition were the first step in image analysis (Figure 1).

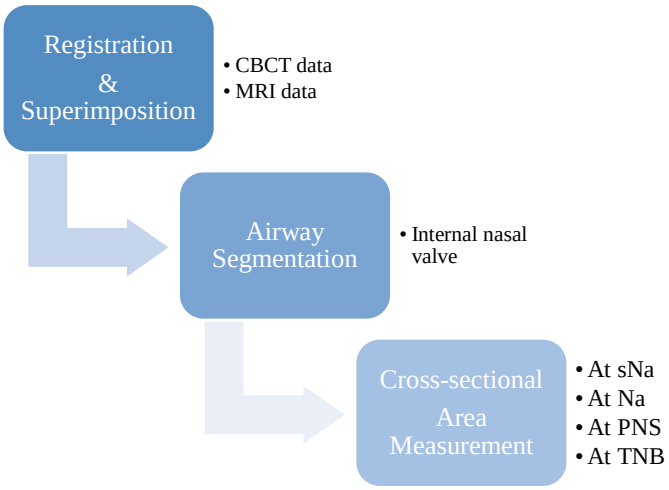

Figure 1. Sequence of workflow.

Segmentation

A threshold tool was used to define the location of the segmentation. To maintain the consistency of the segmentation, a mask was created and used throughout the

segmentation process. The internal nasal valve was isolated using the “paint” tool. All structures that were not the internal nasal valve were removed using the “un-paint” tool, the “ungroup mask” tool and the “smoothing” tool. A 3D model of the internal nasal valve was generated.

Cross-Sectional Area Measurements

After superimposition and segmentation, the cross-sectional area of the internal nasal valve was measured in the coronal plane at three anatomic landmarks: 1) at soft tissue nasion (sNa), at the anterior edge of inferior nasal concha (INC), 2) at nasion (Na), slightly anterior to the inferior nasal concha, and 3) at the posterior nasal spine (PNS), at the posterior edge of the inferior nasal concha (Figure 2).

Additionally, we utilized an alternative method to assess the cross-sectional area of the internal nasal valve in CBCT and MRI. Reformatted scans were constructed in the plane perpendicular to the axis of nasal airflow, using the dorsal surface of the nasal bone as a reference plane, which approximates the acoustic axis, estimated on the sagittal view. We then measured the cross-sectional area of the internal nasal valve at the tip of the nasal bone (TNB) perpendicular to the estimated acoustic axis in the coronal plane (Figure 3).

The area was obtained along the margins of the airway lumen. The area was calculated using the “general statistics” tool. The cross-sectional areas were measured through the same anatomical landmarks on the MRI and CBCT scans and the values were compared.

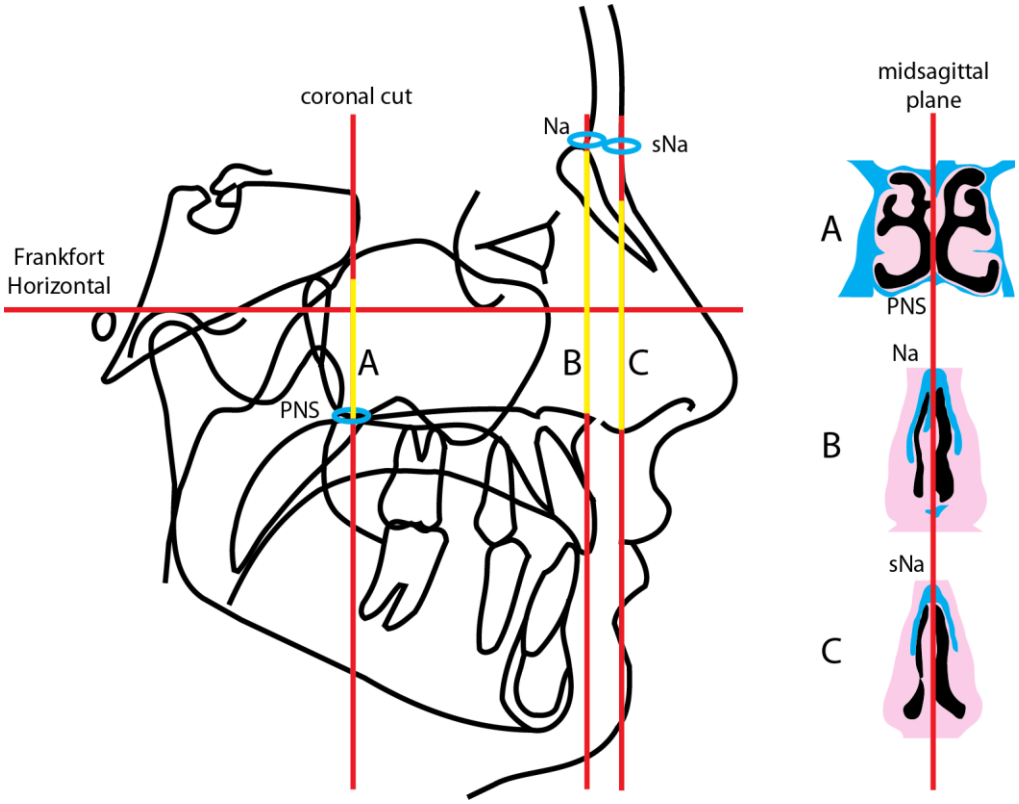

Figure 2. Anatomical landmarks used to measure the cross-sectional area of INV in the coronal plane perpendicular to Frankfort Horizontal. A= INV cross-section at PNS, B= INV cross-section at Na, C= INV cross-section at sNa. The anteroposterior location of the airway cross-section is indicated in yellow.

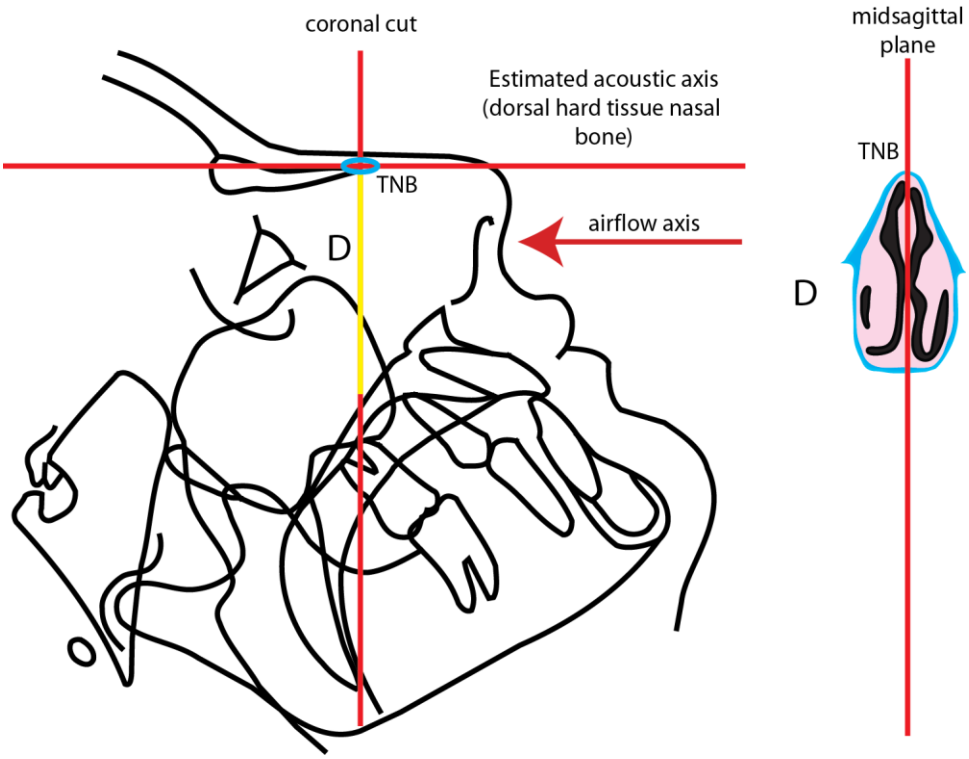

Figure 3. Anatomical landmark used to measure the cross-sectional area of INV in the coronal plane perpendicular to estimated acoustic axis (EAA). D= INV cross-section at TNB. The anteroposterior location of the airway cross-section is indicated in yellow.

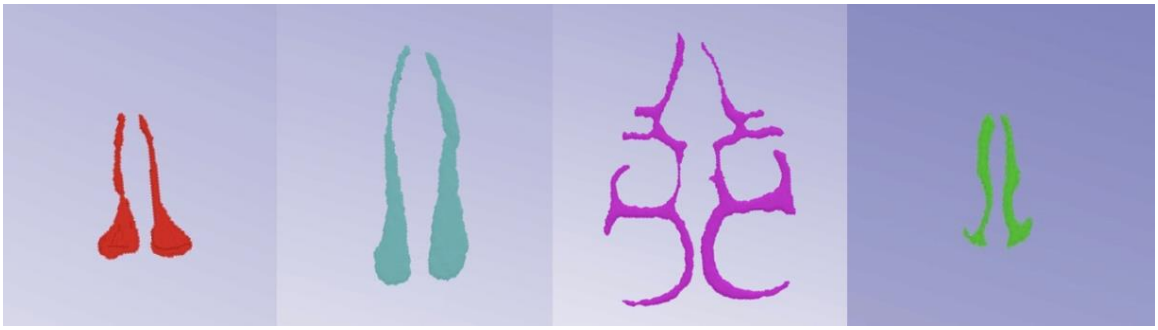

Figure 4. 3D representation of the cross-sectional area of INV at 4 anatomic landmarks. Red= area at sNa, Teal= area at Na, Purple= area at PNS, Green= area at TNB.

Statistical Analysis

SPSS™ (V, 23.0) software (SPSS Inc., Chicago, IL, USA) was used for statistical analysis. One examiner performed all measurements. Agreement between CBCT and MRI measurements was evaluated with an Intraclass Correlation Coefficient (ICC) at an alpha level of 0.05. A 30% random sample of the study's measurements (four sets of measurements) were remeasured by the same operator one month after the initial measurements to determine intra-rater reliability.

Bland-Altman analysis was performed by constructing a scatter plot in which the difference between the paired measurements were plotted on the y-axis and the average of the measures of the two methods on the x-axis. The mean difference in values obtained with the two methods was referred to as the bias and represented by a central horizontal line on the plot. The standard deviation (SD) of differences between the paired measurements was used to construct horizontal lines above and below the central horizontal line to represent 95% limits of agreement (LOA) (mean bias +/- 1.96 SD) and was called upper and lower LOA. The plot allowed us to visually assess the bias, data scatter and the relationship between magnitude of difference and size of measurement.

Results

Overall agreement between the cross-sectional area measurements made on CBCT and MRI was excellent with an ICC of 0.876 (CI 0.833 to 0.908). All CBCT/MRI comparisons at each landmark plane (sNa, Na, PNS, TNB) showed excellent agreement. (Table 1).

Table 1. Stratified Intraclass Correlation Coefficient with 95% confidence level.

Anatomic Landmark	ICC	Lower Bound	Upper Bound	p-Value ($\alpha = 0.05$)
Overall	0.876	0.833	0.908	0.001
sNa	0.953	0.912	0.975	0.001
Na	0.865	0.758	0.927	0.001
PNS	0.822	0.687	0.902	0.001
TNB	0.883	0.789	0.937	0.001

The MRI-CBCT mean differences were calculated for each anatomical landmark (Table 2). No statistically significant differences were observed. The positive mean difference indicated higher values for MRI measurements on average. The negative mean difference was indicative of higher CBCT values.

Table 2. Mean difference (cm^2) of MRI-CBCT valve measurements with 95% confidence level.

Anatomic Landmark	Mean Difference (cm^2)	SD (cm^2)
Overall	-0.001	0.661
sNa	-0.057	0.276
Na	-0.003	0.544
PNS	0.123	0.871
TNB	-0.068	0.801

Bland-Altman plots were used to detect bias and confirm the degree of agreement between the CBCT and MRI measurements (Figures 4-8). The mean difference is the estimated bias. Standard deviation lines demonstrate what should be a random variation around the mean. The heteroscedasticity of the data with values both above and below the delta line confirms the absence of the systematic bias in all types of measurements. The lack of an overall slope formed by the values confirms the absence of proportional bias. The differences between the two imaging modalities was minimal.

The mean difference of cross-sectional areas at sNa when comparing imaging modalities was -0.057 cm^2 indicating slightly higher CBCT values on average at this anatomical landmark (dashed black line in Figure 5).

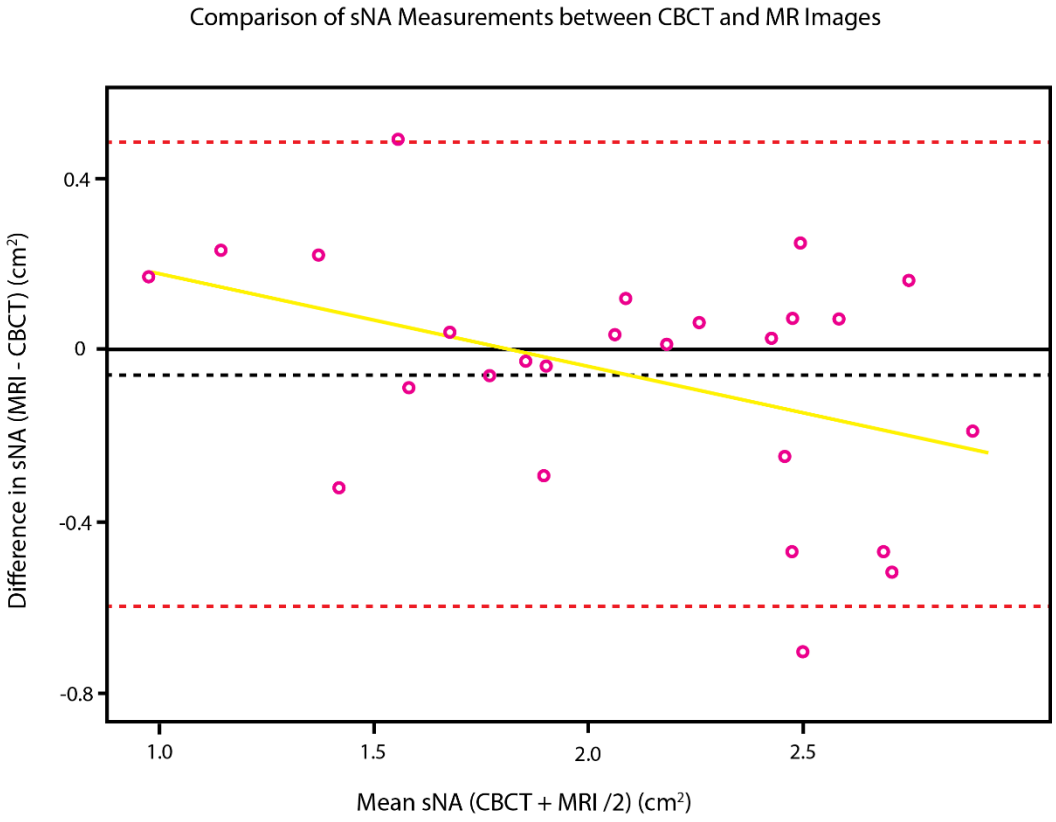

Figure 5. Bland-Altman plot comparing CBCT and MRI cross-sectional area of INV at sNa. The horizontal lines (red dashed lines) represent the 95% confidence interval for the difference between MRI and CBCT measurements. The negative mean difference indicates slightly higher CBCT values (black dashed line). The yellow line indicates the trend of the data.

The mean MRI-CBCT difference of cross-sectional areas at Na was -0.003 cm^2 indicating slightly higher CBCT values (dashed black line in Figure 6).

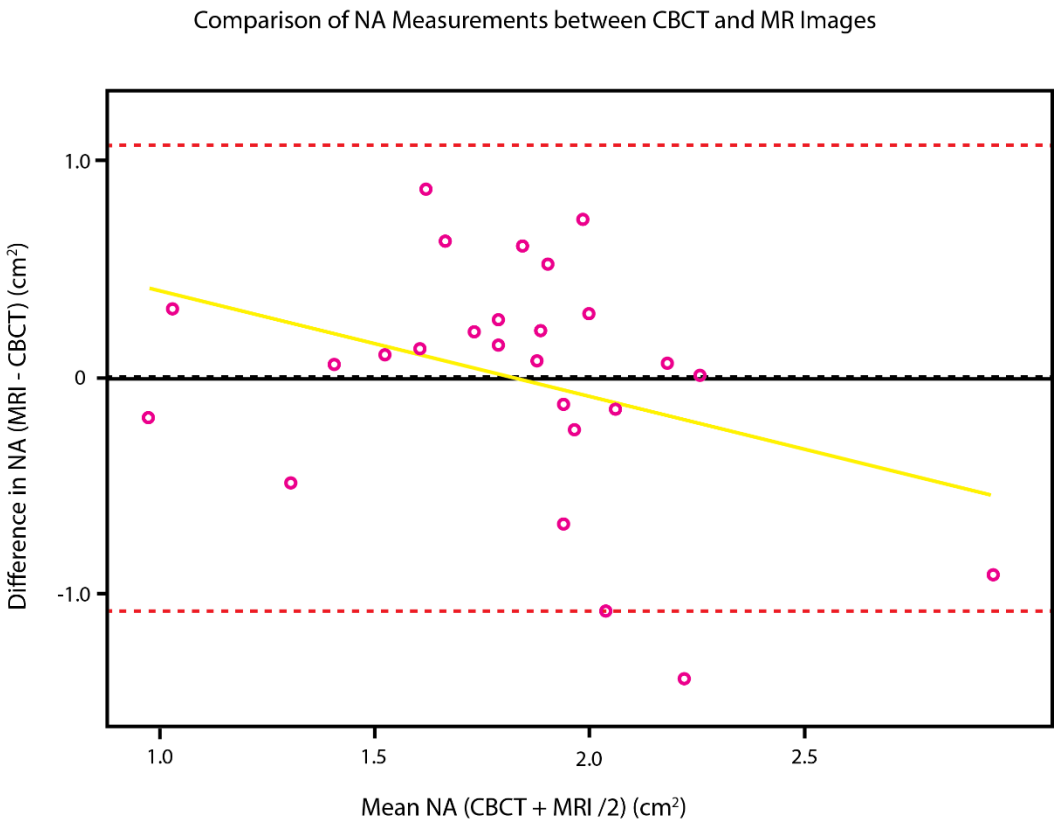

Figure 6. Bland-Altman plot comparing CBCT and MRI cross-sectional area of INV at Na. The horizontal lines (red dashed lines) represent the 95% confidence interval for the difference between MRI and CBCT measurements. The negative mean difference indicates slightly higher CBCT values (black dashed line). The yellow line indicates the trend of the data.

When comparing cross-sectional areas at PNS, the mean MRI-CBCT difference was 0.123 cm^2 indicating slightly higher MRI values at this anatomical landmark (dashed black line in Figure 7).

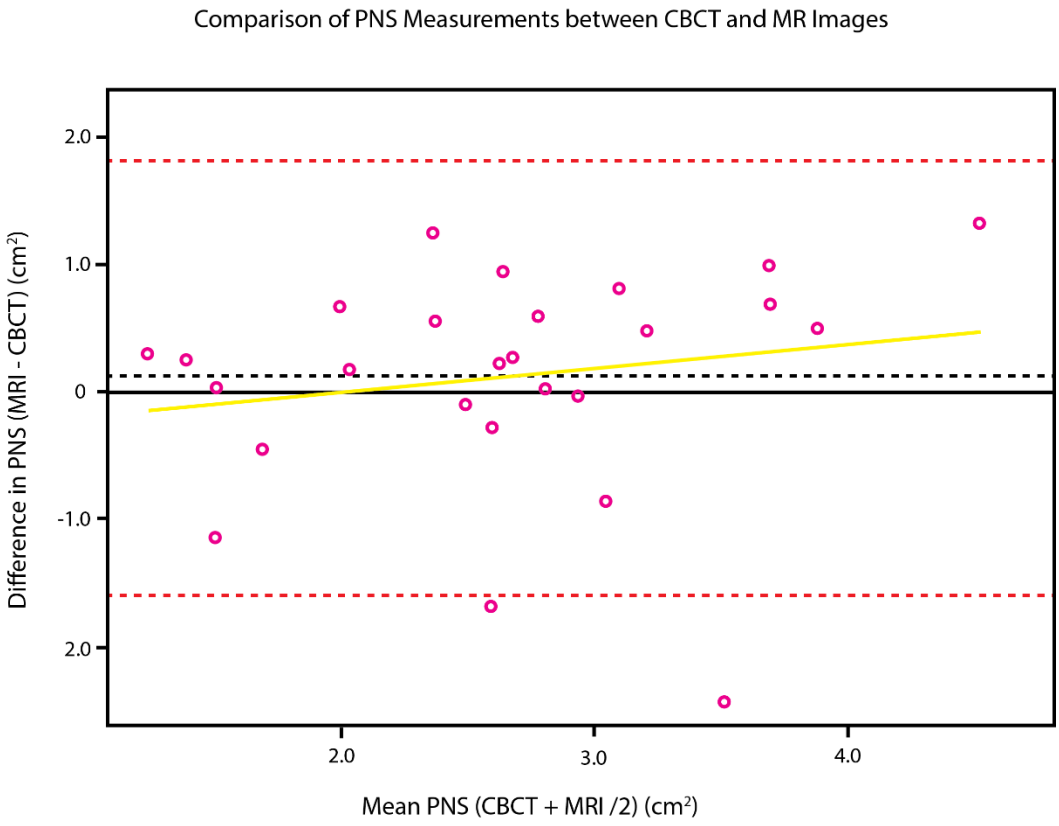

Figure 7. Bland-Altman plot comparing CBCT and MRI cross-sectional area of INV at PNS. The horizontal lines (red dashed lines) represent the 95% confidence interval for the difference between MRI and CBCT measurements. The positive mean difference indicates slightly higher MRI values (black dashed line). The yellow line indicates the trend of the data.

The mean MRI-CBCT difference for cross-sectional areas at TNB was determined to be -0.068 cm^2 indicating slightly higher CBCT values (dashed black line in Figure 8).

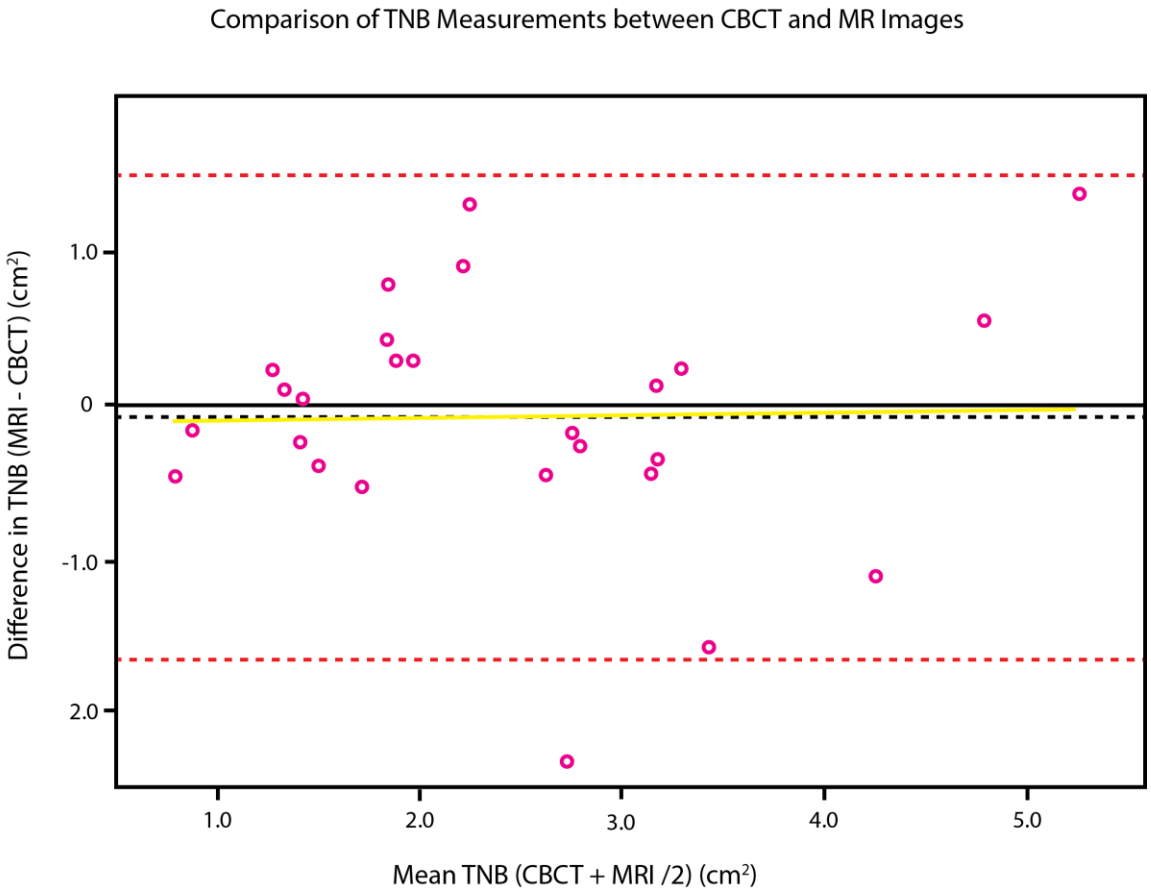

Figure 8. Bland-Altman plot comparing CBCT and MRI cross-sectional area of the INV at TNB. The horizontal lines (red dashed lines) represent the 95% confidence interval for the difference between MRI and CBCT measurements. The negative mean difference indicates slightly higher CBCT values (black dashed line). The yellow line indicates the trend of the data.

The mean MRI-CBCT difference for cross-sectional areas at all anatomical landmarks was determined to be -0.001 cm^2 indicating slightly higher CBCT values (dashed black line in Figure 9).

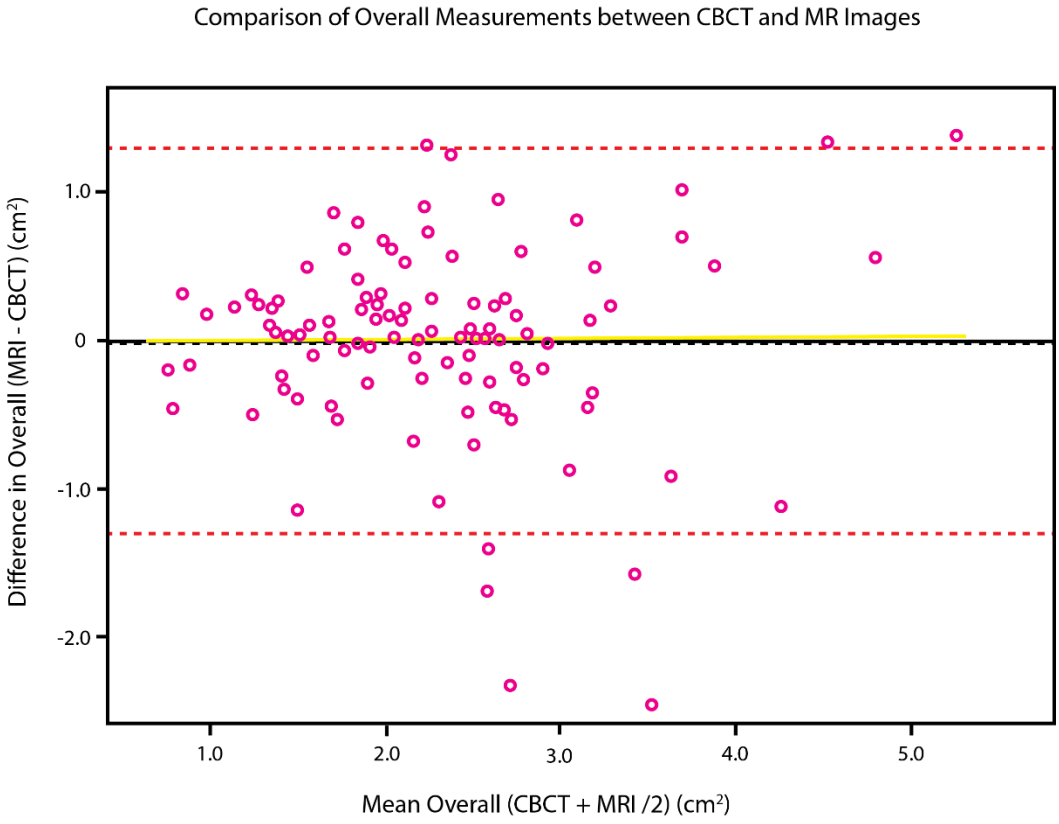

Figure 9. Bland-Altman plot comparing CBCT and MRI cross-sectional area of INV at all anatomical landmarks. The horizontal lines (red dashed lines) represent the 95% confidence interval for the difference between MRI and CBCT measurements. The negative mean difference indicates slightly higher CBCT values (black dashed line). The yellow line indicates the trend of the data.

Reliability was tested by repeating the measurements for four subjects on CBCT and MRI images after a one-month wash-out period. Reliability was very high for both CBCT (Table 3) and MRI (Table 4).

Raw data can be found in appendices A-D.

Table 3. Intra Rater Reliability Intraclass Correlation Coefficient for CBCT.

Anatomic Landmark	ICC	Lower Bound	Upper Bound
Overall	1.00	1.00	1.00
sNa	1.00	1.00	1.00
Na	1.00	0.998	1.00
PNS	1.00	1.00	1.00
TNB	1.00	0.998	1.00

Table 4. Intra Rater Reliability Intraclass Correlation Coefficient for MRI.

Anatomic Landmark	ICC	Lower Bound	Upper Bound
Overall	0.999	0.998	1.00
sNa	1.00	1.00	1.00
Na	1.00	0.999	1.00
PNS	0.998	0.992	0.999
TNB	1.00	1.00	1.00

Discussion

The nasal valve area has been under investigation and measurements have been made with various methods with different modifications. These methods include evaluations by imaging such as CT, MRI, and acoustic rhinometry.[21] Xiong et al., demonstrated that the volume and area of every cross section of the nasal airway can be calculated in an MRI image.[13] However, CBCT remains the preferred imaging modality for evaluating the craniofacial skeleton. Yamashina et al., concluded that CBCT measurements of oropharyngeal air spaces was quite accurate.[27] However, owing to the limited number of adequate studies, comparison of cross-sectional area measurements remains challenging.

A study done by Farina et al., showed that CBCT improves the ability to determine cross-sectional areas of the nares and internal nasal valves bilaterally.[30] The study concluded that the area of both internal nasal valves could be used a reference to establish the minimal cross-sectional area compatible with respiratory health.

A study done by Tai et al. concluded that MRI and CBCT images showed similar linear measurements.[14] The mean differences of the anatomical landmarks of the soft tissue measurements from CBCT and MRI scans ranged from -0.60 to 0.73 mm. A prospective study evaluating the diagnosis of impacted teeth using MRI demonstrated accurate analysis of full volumetric morphology of impacted teeth without exposure to ionizing radiation.[12] Agreement of tooth length measurements on CBCT and MRI were also evaluated.[28] Taylor indicated a high degree of correlation between CBCT (ICC 0.998, $P< 0.001$) and MR images (ICC 0.970, $P<0.001$).[28]

Maspero et al., compared the accuracy and diagnostic capabilities of 3D cephalometric analysis on CBCT to those on MRI to assess whether the latter can deliver a comparable quality of information while avoiding radiation exposure.[29] The results demonstrated that cephalometric measurements on 3T-MRI possess adequate reliability and repeatability and they show satisfying agreement with values measured on CBCT scans. Maspero reported an ICC of 0.957 (CI 0.944 – 0.971) for CBCT and an ICC of 0.833 (CI 0.798-0.868) for MRI. Bland-Altman analysis revealed high levels of agreement between the two modalities for all measurements.[29] These results are similar to the results in this study where the ICC for INV cross-sectional area measurements was 0.876 (CI 0.833-0.908).

The aim of the current study was to determine if 3-Tesla (3T) MR scans are accurate in assessing the cross-sectional area of the internal nasal valve in comparison to CBCT scans. As it accounts for 50% of the total airway resistance, the INV is a significant anatomical area of nasal obstruction, which can have potential clinical implications on the craniofacial skeleton and malocclusion.[30] The results of this study seem to support the potential use of 3T-MRI as a reliable and accurate alternative to CBCT in the evaluation of the nasal airway. Considering the overall good agreement with CBCT and the absence of radiation exposure, 3T-MRI INV area analysis could be performed in the future to reduce radiation, which is important in young patients.[12]

MRI technology may address MRI limitations. Possible solutions may involve adopting short scanning protocols and the use of ceramic and titanium appliances.[29]

The results of this study indicate that use of 3T-MRI for INV analysis is a topic that should be investigated. It is hoped that ionizing radiation can be eliminated in orthodontic treatment planning.

Conclusion

MRI and CBCT give similar cross-sectional area measurements of the internal nasal valve.

References

1. Halazonetis DJ. From 2-dimensional cephalograms to 3-dimensional computed tomography scans. *Am J Orthod Dentofacial Orthop.* May 2005;127(5):627-637.

3. Machado GL. CBCT imaging - A boon to orthodontics. *Saudi Dent J.* Jan 2015;27(1):12-21.

4. Mah JK, Huang JC, Choo H. Practical applications of cone-beam computed tomography in orthodontics. *J Am Dent Assoc.* Oct 2010;141 Suppl 3:7S-13S.

5. Hodges RJ, Atchison KA, White SC. Impact of cone-beam computed tomography on orthodontic diagnosis and treatment planning. *Am J Orthod Dentofacial Orthop.* May 2013;143(5):665-674.

7. Adibi S, Zhang W, Servos T, O'Neill PN. Cone beam computed tomography in dentistry: what dental educators and learners should know. *J Dent Educ.* Nov 2012;76(11):1437-1442.

8. Grunheid T, Kolbeck Schieck JR, Pliska BT, Ahmad M, Larson BE. Dosimetry of a cone-beam computed tomography machine compared with a digital x-ray machine in orthodontic imaging. *Am J Orthod Dentofacial Orthop.* Apr 2012;141(4):436-443.

9. Jaju PP, Jaju SP. Cone-beam computed tomography: Time to move from ALARA to ALADA. *Imaging Sci Dent.* Dec 2015;45(4):263-265.

10. Gray CF, Redpath TW, Smith FW, Staff RT. Advanced imaging: Magnetic resonance imaging in implant dentistry. *Clin Oral Implants Res.* Feb 2003;14(1):18-27.

11. Karatas OH, Toy E. Three-dimensional imaging techniques: A literature review. *Eur J Dent.* Jan 2014;8(1):132-140.

12. Tymofiyeva O, Rottner K, Jakob PM, Richter EJ, Proff P. Three-dimensional localization of impacted teeth using magnetic resonance imaging. *Clin Oral Investig.* Apr 2010;14(2):169-176.

13. Xiong H, Huang X, Li Y, Li J, Xian J, Huang Y. A Method for Accurate Reconstructions of the Upper Airway Using Magnetic Resonance Images. *PLoS One.* 2015;10(6):e0130186.

14. Tai K, Park JH, Hayashi K, et al. Preliminary study evaluating the accuracy of MRI images on CBCT images in the field of orthodontics. *J Clin Pediatr Dent.* Winter 2011;36(2):211-218.

21. Yoshinami H, Kase Y, Iinuma T. [Evaluation of nasal valve by CT imaging]. *Nihon Jibiinkoka Gakkai Kaiho.* Jan 2001;104(1):24-32.

27. Yamashina A, Tanimoto K, Sutthiprapaporn P, Hayakawa Y. The reliability of computed tomography (CT) values and dimensional measurements of the oropharyngeal region using cone beam CT: Comparison with multidetector CT. *Dentomaxillofac Radiol* 2008;37:245-51

28. Taylor A. Correlation of Tooth Length Measurements made on CBCT and 3T MR Images. *Loma Linda University Electronic Theses, Dissertations & Projects*. 2016

29. Maspero, Cinzia, et al. "Comparison of a Tridimensional Cephalometric Analysis Preformed on 3T-MRI Compared with CBCT: a Pilot Study in Adults." *Progress in Orthodontic*, vol. 20, no. 1, 2019.

30. Farina, Rodrigo, et al. "Relationship Between Nostril, Nasal Valve and Minimal Cross-Sectional Area in Functional Upper Airway." *Journal of Craniofacial Surgery*, vol. 30, no. 7, 2019, pp. 2202-2206.

CHAPTER THREE

EXTENDED DISCUSSION

Limitations of the Study

There are several limitations in this study. First, the sample was relatively small and included only thirteen subjects. There is also heterogeneity in the small sample, which could produce an outsized effect on the variability of the measurements. Another limitation is the difficulty in distinguishing between air and tissue when utilizing the software threshold tool. Filling the airway space was subjective since it solely relied on visual determination by the examiner. Currently, there is no standardized modality of selecting the threshold value to acquire the actual cross-sectional area. A third limitation is the complexity of the software used to make the measurements. Utilizing the software required extensive training and a learning curve is apparent in the statistical analysis. CBCT and MRI agreement improved with the repeated subsample compared to the original sample. This illustrates the learning curve with the progressive use of the software and recognition of the MRI image. Additionally, the limited experience of the operator in determining the anatomical landmarks on MRI images poses another limitation. The high degree of intra-rater reliability indicates adequate calibration of the examiner.

Recommendation for Future Studies

Further studies with larger samples should be conducted to support our findings and to assess whether MRI could be used for airway analysis instead of CBCT. In order

to evaluate MRI's future value as a potential orthodontic diagnostic tool with the possibility of becoming the gold standard imaging modality, further studies need to be performed. Standardized and more precise methods for registration and image segmentation need to be established to generate accurate and repeatable MRI data. Moreover, studies examining the cost-benefit relationship between CBCT and MRI should be evaluated to understand MRI's value in orthodontic diagnosis and treatment planning.

References

1. Halazonetis DJ. From 2-dimensional cephalograms to 3-dimensional computed tomography scans. *Am J Orthod Dentofacial Orthop.* May 2005;127(5):627-637.

2. Mozzo P, Procacci C, Tacconi A, Martini PT, Andreis IA. A new volumetric CT machine for dental imaging based on the cone-beam technique: preliminary results. *Eur Radiol.* 1998;8(9):1558-1564.

3. Machado GL. CBCT imaging - A boon to orthodontics. *Saudi Dent J.* Jan 2015;27(1):12-21.

4. Mah JK, Huang JC, Choo H. Practical applications of cone-beam computed tomography in orthodontics. *J Am Dent Assoc.* Oct 2010;141 Suppl 3:7S-13S.

5. Hodges RJ, Atchison KA, White SC. Impact of cone-beam computed tomography on orthodontic diagnosis and treatment planning. *Am J Orthod Dentofacial Orthop.* May 2013;143(5):665-674.

6. Ludlow JB, Gubler M, Cevidanes L, Mol A. Precision of cephalometric landmark identification: cone-beam computed tomography vs conventional cephalometric views. *Am J Orthod Dentofacial Orthop.* Sep 2009;136(3):312 e311-310; discussion 312-313.

7. Adibi S, Zhang W, Servos T, O'Neill PN. Cone beam computed tomography in dentistry: what dental educators and learners should know. *J Dent Educ.* Nov 2012;76(11):1437-1442.

8. Grunheid T, Kolbeck Schieck JR, Pliska BT, Ahmad M, Larson BE. Dosimetry of a cone-beam computed tomography machine compared with a digital x-ray machine in orthodontic imaging. *Am J Orthod Dentofacial Orthop.* Apr 2012;141(4):436-443.

9. Jaju PP, Jaju SP. Cone-beam computed tomography: Time to move from ALARA to ALADA. *Imaging Sci Dent.* Dec 2015;45(4):263-265.

10. Gray CF, Redpath TW, Smith FW, Staff RT. Advanced imaging: Magnetic resonance imaging in implant dentistry. *Clin Oral Implants Res.* Feb 2003;14(1):18-27.

11. Karatas OH, Toy E. Three-dimensional imaging techniques: A literature review. *Eur J Dent.* Jan 2014;8(1):132-140.

12. Tymofiyeva O, Rottner K, Jakob PM, Richter EJ, Proff P. Three-dimensional localization of impacted teeth using magnetic resonance imaging. *Clin Oral Investig.* Apr 2010;14(2):169-176.

13. Xiong H, Huang X, Li Y, Li J, Xian J, Huang Y. A Method for Accurate Reconstructions of the Upper Airway Using Magnetic Resonance Images. *PLoS One.* 2015;10(6):e0130186.

14. Tai K, Park JH, Hayashi K, et al. Preliminary study evaluating the accuracy of MRI images on CBCT images in the field of orthodontics. *J Clin Pediatr Dent.* Winter 2011;36(2):211-218.

15. Defabjanis P. Impact of nasal airway obstruction on dentofacial development and sleep disturbances in children: preliminary notes. *J Clin Pediatr Dent.* Winter 2003;27(2):95-100.

16. Lopatiene K, Babarskas A. [Malocclusion and upper airway obstruction]. *Medicina (Kaunas).* 2002;38(3):277-283.

17. Principato JJ. Upper airway obstruction and craniofacial morphology. *Otolaryngol Head Neck Surg.* Jun 1991;104(6):881-890.

18. Ribault JY, Fourestier J, Gacon J, Renon P. [Results of the evaluation of nasal respiration in maxillo-mandibular malocclusion in children. Apropos of 53 cases]. *Rev Stomatol Chir Maxillofac.* 1990;91 Suppl 1:96-98.

19. Murthy VA, Reddy RR, Pragadeeswaran K. Internal nasal valve and its significance. *Indian J Otolaryngol Head Neck Surg.* Aug 2013;65(Suppl 2):400-401.

20. Bloom JD, Sridharan S, Hagiwara M, Babb JS, White WM, Constantinides M. Reformatted computed tomography to assess the internal nasal valve and association with physical examination. *Arch Facial Plast Surg.* Sep-Oct 2012;14(5):331-335.

21. Yoshinami H, Kase Y, Iinuma T. [Evaluation of nasal valve by CT imaging]. *Nihon Jibiinkoka Gakkai Kaiho.* Jan 2001;104(1):24-32.

22. Moche JA, Cohen JC, Pearlman SJ. Axial computed tomography evaluation of the internal nasal valve correlates with clinical valve narrowing and patient complaint. *Int Forum Allergy Rhinol.* Jul 2013;3(7):592-597.

23. Rojas E, Corvalan R, Messen E, Sandoval P. Upper airway assessment in Orthodontics: a review. *Odontoestomatología*. 2017;19(30).

24. Shah A. Use of MRI in Orthodontics - A Review. *Journal of Imaging and Interventional Radiology*. 2017;01(01:3).

25. Shia Ng L, Lo S. Management of the Internal Nasal Valve. *Otorhinolaryngology Clinics - An International Journal*. 2013;5:43-45.

26. Veron A, Bocquet J, Clareton V, et al. Value of CT scan measures of the nasal valve for predicting clinical nasal obstruction. *European Society of Radiology*. 2011.

27. Yamashina A, Tanimoto K, Sutthiprapaporn P, Hayakawa Y. The reliability of computed tomography (CT) values and dimensional measurements of the oropharyngeal region using cone beam CT: Comparison with multidetector CT. *Dentomaxillofac Radiol* 2008;37:245-51

28. Taylor A. Correlation of Tooth Length Measurements made on CBCT and 3T MR Images. *Loma Linda University Electronic Theses, Dissertations & Projects*. 2016

29. Maspero, Cinzia, et al. "Comparison of a Tridimensional Cephalometric Analysis Preformed on 3T-MRI Compared with CBCT: a Pilot Study in Adults." *Progress in Orthodontic*, vol. 20, no. 1, 2019.

30. Farina, Rodrigo, et al. "Relationship Between Nostril, Nasal Valve and Minimal Cross-Sectional Area in Functional Upper Airway." *Journal of Craniofacial Surgery*, vol. 30, no. 7, 2019, pp. 2202-2206.

APPENDIX A
INV MEASUREMENTS (CM^2) MADE ON MRI SCANS

right	MRI		left	MRI		total	MRI
sNA	2.37		**sNA**	2.67		**sNA**	5.04
	2.42			2.44			4.86
	2.03			2.23			4.26
	2.92			1.87			4.79
	1.63			2.04			3.67
	1.66			1.80			3.46
	2.04			2.97			5.01
	2.18			1.92			4.10
	2.71			2.85			5.56
	1.31			1.26			2.57
	1.03			0.89			1.92
	2.99			1.58			4.57
	2.58			2.55			5.13
right	**MRI**		**left**	**MRI**		**total**	**MRI**
NA	2.42		**NA**	2.63		**NA**	5.05
	2.50			1.85			4.35
	1.99			2.33			4.32
	4.09			2.85			6.94
	0.85			0.68			1.53
	2.23			1.87			4.10
	1.76			3.28			5.04
	1.73			1.61			3.34
	2.04			2.50			4.54
	1.36			1.48			2.84
	1.27			1.82			3.09
	2.12			1.51			3.63
	1.88			1.46			3.34
right	**MRI**		**left**	**MRI**		**total**	**MRI**
PNS	2.09		**PNS**	1.74		**PNS**	3.83

INV MEASUREMENTS (CM^2) MADE ON MRI SCANS (CONTINUED)

	4.73			2.96			7.69
	2.94			3.43			6.37
	3.63			3.35			6.98
	1.95			1.66			3.61
	1.26			1.09			2.35
	2.48			2.79			5.27
	2.17			2.51			4.68
	3.86			3.19			7.05
	1.91			2.07			3.98
	1.49			2.74			4.23
	2.54			3.48			6.02
	2.69			2.54			5.23
right	**MRI**		**left**	**MRI**		**total**	**MRI**
TNB	1.59		**TNB**	1.63		**TNB**	3.22
	3.37			4.21			7.58
	3.88			3.17			7.05
	3.35			4.81			8.16
	1.17			0.96			2.13
	1.69			1.53			3.22
	2.92			2.84			5.76
	1.45			1.77			3.22
	4.52			4.57			9.09
	1.28			1.03			2.31
	1.41			1.99			3.40
	3.10			2.85			5.95
	1.82			1.74			3.56

APPENDIX B
REPEATED INV MEASUREMENTS (CM^2) MADE ON MRI SCANS

right	MRI		left	MRI		total	MRI
sNA	1.64		**sNA**	1.81		**sNA**	3.45
	1.02			0.90			1.92
	3.01			1.61			4.62
	2.56			2.55			5.11
right	**MRI**		**left**	**MRI**		**total**	**MRI**
NA	2.22		**NA**	1.86		**NA**	4.08
	1.28			1.85			3.13
	2.13			1.50			3.63
	1.87			1.49			3.36
right	**MRI**		**left**	**MRI**		**total**	**MRI**
PNS	1.31		**PNS**	1.30		**PNS**	2.61
	1.49			2.74			4.23
	2.55			3.50			6.05
	2.69			2.55			5.24
right	**MRI**		**left**	**MRI**		**total**	**MRI**
TNB	1.70		**TNB**	1.53		**TNB**	3.23
	1.40			2.00			3.40
	3.08			2.87			5.95
	1.79			3.70			5.49

APPENDIX C
INV MEASUREMENTS (CM^2) MADE ON CBCT SCANS

right	**CBCT**		**left**	**CBCT**		**total**	**CBCT**
sNA	2.62		**sNA**	2.83		**sNA**	5.45
	2.45			2.51			4.96
	2.15			2.29			4.44
	2.45			1.84			4.29
	1.54			2.08			3.62
	1.70			1.74			3.44
	1.75			2.45			4.20
	2.19			1.88			4.07
	2.24			2.15			4.39
	1.80			1.48			3.28
	1.26			1.06			2.32
	2.80			1.26			4.06
	2.33			2.62			4.95
right	**CBCT**		**left**	**CBCT**		**total**	**CBCT**
NA	2.27		**NA**	2.64		**NA**	4.91
	1.83			2.37			4.20
	2.20			2.09			4.29
	3.18			1.77			4.95
	0.66			0.99			1.65
	2.11			2.02			4.13
	1.97			1.89			3.86
	2.33			1.74			4.07
	2.11			2.56			4.67
	1.41			0.99			2.40
	2.13			2.08			4.21
	2.40			1.61			4.01
	2.60			2.08			4.68
right	**CBCT**		**left**	**CBCT**		**total**	**CBCT**
PNS	2.66		**PNS**	2.99		**PNS**	5.65

INV MEASUREMENTS (CM^2) MADE ON CBCT SCANS (CONTINUED)

	2.30			3.45			5.75
	2.92			1.75			4.67
	4.13			4.04			8.17
	2.12			2.33			4.45
	1.52			1.39			2.91
	3.08			2.82			5.90
	3.11			2.74			5.85
	5.19			4.20			9.39
	1.46			0.93			2.39
	1.52			2.46			3.98
	2.44			2.62			5.06
	3.50			2.82			6.32
right	**CBCT**		**left**	**CBCT**		**total**	**CBCT**
TNB	2.90		**TNB**	2.05		**TNB**	4.95
	2.93			2.65			5.58
	1.57			3.41			4.98
	3.00			3.70			6.70
	1.39			0.80			2.19
	1.30			1.29			2.59
	2.66			2.66			5.32
	2.24			2.67			4.91
	5.07			5.94			11.01
	1.38			0.57			1.95
	1.45			1.46			2.91
	3.23			2.40			5.63
	2.12			2.04			4.16

APPENDIX D
REPEATED INV MEASUREMENTS (CM^2) MADE ON CBCT SCANS

right	CBCT		left	CBCT		total	CBCT
sNA	1.71		**sNA**	1.74		**sNA**	3.45
	1.26			1.04			2.30
	2.81			1.24			4.05
	2.36			2.62			4.98
right	**CBCT**		**left**	**CBCT**		**total**	**CBCT**
NA	2.12		**NA**	1.99		**NA**	4.11
	2.18			2.08			4.26
	2.42			1.62			4.04
	2.62			2.10			4.72
right	**CBCT**		**left**	**CBCT**		**total**	**CBCT**
PNS	1.52		**PNS**	1.38		**PNS**	2.90
	1.55			2.44			3.99
	2.45			2.62			5.07
	3.49			2.85			6.34
right	**CBCT**		**left**	**CBCT**		**total**	**CBCT**
TNB	1.31		**TNB**	1.30		**TNB**	2.61
	1.44			1.51			2.95
	3.22			2.45			5.67
	2.12			2.06			4.18